

Elaboration and Characterization of Soy/Zein Protein Microspheres for Controlled Nutraceutical Delivery

Lingyun Chen and Muriel Subirade*

Chaire de recherche du Canada sur les protéines, les bio-systèmes et les aliments fonctionnels, Institut de recherche sur les nutraceutiques et les aliments fonctionnels (INAF/STELA), Faculté des sciences de l'agriculture et de l'alimentation, Université Laval, Pavillon Paul Comtois, Sainte-Foy, Québec, G1K 7P4 Canada

Received August 29, 2009; Revised Manuscript Received October 29, 2009

Microspheres (15–25 μm) of soy protein isolate (SPI), zein, and SPI/zein blends were prepared using a cold gelation method as possible delivery systems for nutraceutical products. Microsphere matrix crystalline structure, swelling behavior, and nutrient load release kinetics in simulated gastrointestinal fluids were investigated. SPI microspheres showed early burst release of the model nutrient, whereas zein microspheres showed very slow release in both simulated gastric and intestinal fluids. Blending of SPI and zein provides a convenient method of adjusting the hydrophobicity and crystallinity of the protein matrix and hence its swelling behavior and in vivo nutrient release kinetics. Diffusion plays a major role in regulating nutrient release. SPI/zein microspheres blended at ratios of 5:5 and 3:7 showed near zero-order release kinetics over the test period in simulated intestinal buffer and thus have potential as delivery vehicles for nutraceutical products in functional foods.

1. Introduction

Interest in delivery systems for nutraceutical products has recently been growing because of the emergence of vitamins, probiotics, and bioactive peptides believed to confer health benefits, in particular, when consumed as active ingredients in so-called functional foods. The type of material used to encapsulate the active ingredient and the physicochemical properties of this material are the most critical determinants of the functionality of these food systems.¹ Although numerous synthetic polymers have been used to formulate intelligent, modulated, and selective drug delivery systems to maximize drug action and minimize side effects in biomedical and pharmaceutical applications,^{2,3} these materials are seldom generally recognized as safe (GRAS) for food use. Food proteins are therefore attracting the attention of scientists and industry as possible encapsulation materials for nutraceutical compounds. These GRAS materials are obtained from abundant natural sources and are widely used in formulated foods because they have high nutritional value and are degradable by digestive enzymes. They have excellent emulsifying and gelling properties and allow the formation of hydrogels or hydrogel emulsions with controllable droplet size. Furthermore, they interact strongly with various types of nutraceutical compounds via hydrogen bonding, hydrophobic bonding, and electrostatic interactions, thus stabilizing them in the protein network.^{4–7} We have previously developed microparticles and nanoparticles of various formulations of whey protein either alone or combined with other biopolymers.^{8–11} These displayed the desirable properties of protecting nutraceutical compounds in the stomach and releasing them in the intestinal environment.

Soy protein isolate (SPI) is a plant protein obtained from an abundant, inexpensive, and renewable resource. It is composed almost exclusively of two globular protein fractions called 7S (*b*-conglycinin) and 11S (glycinin).¹² Traditionally, heating is

required to induce soy protein gelation. We recently developed a cold gelation method for producing soy protein hydrogels at ambient temperature.¹³ Already widely practiced with whey proteins,¹⁴ this process consists of two distinct steps. During the preheating step, proteins are unfolded and polymerized into soluble aggregates, followed by a cooling step and subsequent addition of calcium to form protein networks.¹⁵ This new method provides the opportunity to develop soy-protein-based delivery systems that incorporate heat-sensitive nutraceutical products for food applications.¹⁶ However, research on soy-protein-based microparticles is limited to a handful of articles,^{17,18} and soy protein microparticle formation using the cold gelation method has never been reported. Furthermore, the release properties of soy protein hydrogel matrices have not been characterized in detail.

Microencapsulation in the food industry is done mainly to mask the unpleasant smell and taste of certain compounds in nutraceutical preparations and to protect them during food processing and storage.^{19,20} However, efforts to develop controlled release vehicles to maintain nutraceutical payloads at optimal concentration in vivo are limited. The original purpose of the present research was to study the feasibility of using the cold gelation method to prepare soy protein microparticles that can maintain nutrient release over a 4–6 h period and thereby mimic an administration schedule corresponding to the digestion of a food product. In preliminary experiments, microspheres 15–20 μm in diameter were formed. However, these shed their riboflavin load within 15 min because of the inherent hydrophilic nature of soy protein. We therefore turned to blending food proteins to improve the nutrient release profile of the particles, and zein was chosen for this purpose because it is hydrophobic and obtained from a very abundant source. In this article, we describe the swelling properties of soy/zein microspheres and the kinetics of nutrient release from them in simulated gastrointestinal fluids and discuss the mechanisms of release.

* To whom correspondence should be addressed. Tel: +1-418-656 2131 ext. 4278. Fax: +1-418-656 3353. E-mail: Muriel.subirade@fsaa.ulaval.ca.

2. Materials and Methods

2.1. Materials. Native SPI, obtained from Protient (St. Paul, MN), contained 94.4% protein on a dry basis, as measured by the macro-Kjeldahl method (AOAC 1984) using N-factor 6.25. Soybean oil used to form the emulsions was purchased locally (Merit Selection Brand, Canada). Calcium carbonate (40 nm) was kindly provided by Nano-Materials Technology (Singapore). Zein/pepsin 1:60 000 (from porcine stomach mucosa, crystallized, and lyophilized), Span 80, Tween 80, and riboflavin were purchased from the Sigma Chemical (St. Louis, MO). Pancreatin 5 \times (from hog pancreas) was purchased from ICN Nutritional Biochemicals (Cleveland, OH). All other chemicals were reagent grade.

2.2. Protein Microsphere Preparation. On the basis of preliminary trials, heating SPI solutions at concentrations $\geq 10\%$ (w/w) or close to the isoelectric pH (4.76) resulted in the formation of a 3D network, whereas 6–8% did not yield particles with sufficient strength. A 9.5% (w/w) SPI solution was therefore prepared in double-distilled water by mixing for 1 h at room temperature using a magnetic stirrer. The solution pH was then adjusted to 7.0 using 0.1 M NaOH, placed in tightly closed tubes to avoid evaporation and heated in a 50:50 water/ethylene glycol bath for 30 min at 105 °C, a temperature shown previously by differential scanning calorimetry to denature SPI. The samples were then removed from the bath and cooled to room temperature (25 °C). Zein powder was dispersed in water at pH 11 and stirred to form a 10% (w/w) solution and was not heated. Protein microspheres were prepared using the emulsification/internal gelation technique, as reported previously.¹⁰ In brief, SPI and zein solutions were combined in the ratios shown in the Supporting Information (Section S1). Riboflavin was dispersed in 20 mL of protein solution to form a nutrient/protein aqueous phase. Calcium carbonate was then added to obtain the equivalent of 50 mM Ca²⁺ (except in the case of zein without SPI). This mixture was dispersed in 100 mL of soybean oil in the presence of 1% Span 80 and the oil/solution mixture was homogenized using an Ultra-Turrax homogenizer (Janke & Kunkel, IKALabortechnik, Germany). Then, 60 μ L of glacial acetic acid was added to initiate droplet gelation. After 20 min, the suspension of gel particles in oil was slowly mixed with 150 mL of 50 mM calcium chloride solution. After complete partitioning of gel particles (i.e., microspheres) to the aqueous phase, the oil was discarded, and the particles were filtered and washed thoroughly with 1% (v/v) Tween 80 solution and then lyophilized (model Freezone 4.5, Labconco, Kansas City, MI) and weighed.

2.3. Microsphere Characterization. For size and size distribution analysis, freshly prepared protein microspheres were dispersed in distilled water containing 1% v/v Tween 80 (filtered through a 0.2 mm filter). Static light scattering was measured using a Mastersizer 2000 (Malvern Instruments, Southborough, MA). All size measurements were performed at a 90° scattering angle at 25 °C with 180 s of recording. The mean hydrodynamic diameter was generated by cumulative analysis.

Features such as shape and structure of isolated microspheres were observed using an Olympus BX50WI optical microscope (Olympus, Melville, NY) fitted with epi-fluorescence and optical fluorescent filters (Chroma Technology Corp, Rockingham) and a digital camera (model U-TV1 X, Olympus Optical, Tokyo, Japan). For fluorescence observation, microspheres were stained with phen green. Microsphere morphology was also characterized by scanning electron microscopy (SEM). Each sample was air-dried and viewed at 15 kV using a JEOL JSM 35CF electron microscope.

Infrared spectra of dried protein or dried microsphere were recorded with a Magna 560 Nicolet spectrometer (Madison, WI) equipped with an attenuated total reflectance (ATR) accessory. To study the amide I region of the protein, Fourier self-deconvolutions were performed using the software provided with the spectrometer (Omnicon software). Band narrowing was achieved with a full width at half maximum of 24 cm⁻¹ and with a resolution enhancement factor of 2.5 cm⁻¹.

The microspheres and the native proteins in powder form were also analyzed by X-ray diffraction (XRD). Patterns were recorded using a diffractometer (D5000, Siemens) and Cu K α radiation ($\lambda = 1.5406$ Å) with a 0.1° step scan from 5 to 45° in 2 θ angle.

2.4. Microsphere Swelling Properties. Dry microspheres (100 mg) were placed in buffered solution (0.02 M phosphate containing 0.13 M NaCl) at pH 4.8 (near the pI of soy protein) and at 7.5 (intestinal pH) or in HCl solution at pH 1.2 (gastric pH). Temperature was maintained at 37 °C in an incubator. After swelling reached equilibrium, the suspension was centrifuged at 5000 rpm for 20 min at 23 °C (GSA rotor, model RC5C Sorvall Instruments Dupont, Newton, CT). The supernatant was then removed, and the swollen microspheres were weighed. Microsphere swelling at equilibrium was determined from the weight change before and after swelling

$$\text{percent swelling at equilibrium} = [(W_w - W_d)/W_d] \times 100 \quad (1)$$

where W_w and W_d represent the weights of wet and dry samples, respectively.

2.5. Determination of Riboflavin Loading. To determine riboflavin loading, about 30 mg of dry microspheres was weighed with precision and hydrolyzed in 25 mL of simulated intestinal fluid USP XXII with 1.0% pancreatin (w/v) at 37 °C and pH 7.4 with vigorous agitation for 6 h. The resulting mixture was centrifuged at 12 000 rpm for 20 min at 23 °C (GSA rotor, model RC5C Sorvall Instruments Dupont, Newton, CT). Riboflavin concentration in the supernatant was determined from absorbance at 445 nm measured with a UV–visible spectrophotometer (model 8435, Hewlett-Packard, Palo Alto, CA) and using a standard curve. The riboflavin encapsulation efficiency (EE) and loading efficiency (LE) were calculated as follows: $EE = A/B \times 100$ and $LE = A/C \times 100$, where A is the amount of riboflavin encapsulated in the microspheres, B is the total amount of riboflavin, and C is the total dry weight of the microspheres.

2.6. In Vitro Release Studies. We determined riboflavin release by stirring a suspension of microspheres containing ~ 3 mg of riboflavin in 30 mL of medium using a magnetic bar (at 100 rpm) at 37 °C. The release media were HCl solution at pH 1.2 and phosphate-buffered saline at pH 7.4. Samples (1 mL) withdrawn at 0.5 or 1 h intervals were centrifuged, and we determined the riboflavin content of the supernatant by measuring absorbance at 445 nm. An equal volume of medium was added to the release mixture after each sampling to maintain a constant volume.

2.7. Statistical Analysis. All experiments were performed at least in triplicate. Error bars on graphs represent standard errors obtained from the statistical model. Statistical comparisons were made using the Student t test and analysis of variance (ANOVA). The level of significance used was $p < 0.05$.

3. Results and Discussion

3.1. Microsphere Preparation, Size, and Morphology. The emulsifying, internal cold gelling method adapted from our previous work for the preparation of whey protein microspheres¹⁰ was used to prepare SPI, SPI/zein, or zein microparticles. A 30 min heating step at 105 °C is required in the case of SPI, during which proteins are denatured and polymerize into aggregates, which remain in solution even after cooling. Calcium carbonate is then added to provide the Ca²⁺ necessary to cause the soluble aggregates to form a gel network at the appropriate time. This mixture is then dispersed in soybean oil to form a W/O emulsion, and the glacial acetic acid added in this stage partitions to the droplet phase to free the calcium. Gelation thus occurs within the droplets under controlled conditions of dispersion, making it possible to form particles of various sizes ranging from several to several hundred micrometers. Photographs of SEM images (Figure 1a) show the spherical shape

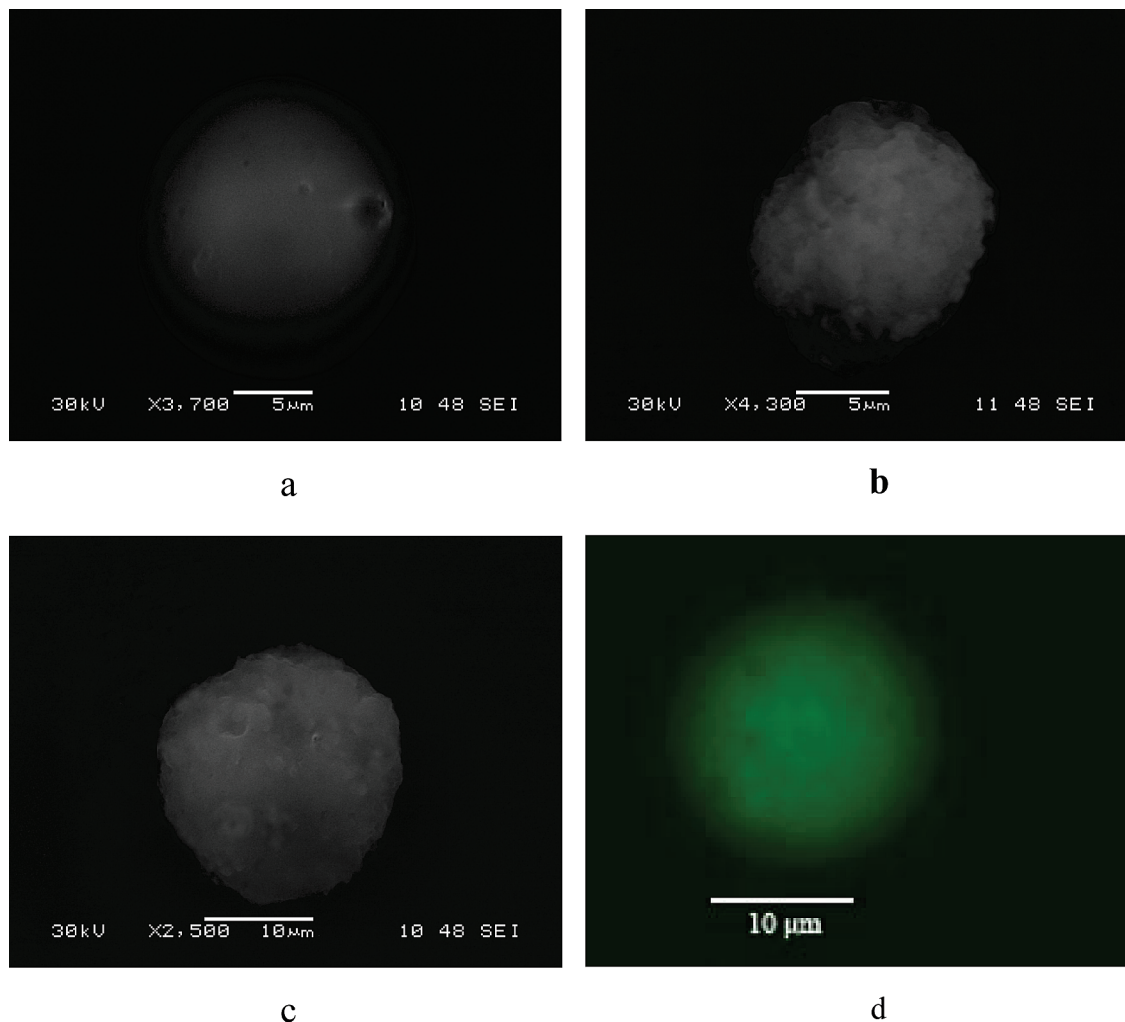


Figure 1. Photographs of (a) pure SPI microspheres, (b) pure zein microspheres, and (c) SPI/zein-3 microspheres viewed by scanning electron microscopy and (d) SPI/zein-3 microspheres labeled with phen green viewed by fluorescence optical microscope.

and very smooth surface of SPI microparticles (labeled as SPI) about 15 μm in diameter. This is the first report of soy protein microspheres prepared at ambient temperature without using toxic or expensive cross-linking reagents such as glutaraldehyde and transglutaminase.^{18,21} This should broaden the range of soy protein uses to include microencapsulation of heat-sensitive bioactive compounds for food or pharmaceutical applications.

Zein microspheres were prepared using essentially the same procedure, except that no thermal denaturing step was done and no calcium carbonate was added. Zein is soluble in alkaline solution but becomes insoluble when the pH is decreased to neutrality, making these two steps unnecessary. The amount of acetic acid added brought the pH down to 6.0.

Microsphere volume mean diameters are summarized in the Supporting Information (Section S1). All protein particles had diameters of about 15–25 μm with relatively narrow distributions. SEM photographs show that they are spherical in shape with smooth surface in general, except for SPI-zein-4 and pure zein microspheres, which display rough surfaces (Figure 1b,c). This may be attributed to the surface crack when dried from solution because of rigidity and brittleness of zein at room temperature^{22,23} and its hydrophobic nature. Actually, it is usually possible upon drying to obtain a very smooth surface with most water-soluble proteins. However, zein always yields relatively rough surface.²⁴ It should be noted that no phase separation was observed for SPI/zein microspheres, suggesting

good miscibility between SPI and zein. Microspheres were also observed using fluorescence microscopy, which allows distinguishing of components inside individual spheres. Using phen green, a fluorescent dye that binds divalent cations, a uniform color was observed (Figure 1d), confirming that Ca^{2+} -linked soy protein gel was distributed homogeneously throughout the microsphere matrix.

3.2. Molecular Structure Characterization. Figure 2 presents FTIR spectra of the amide I region for the protein microspheres as well as SPI and zein in their native form, denatured form, or both.

For native SPI, the amide I band is composed of at least five absorbance peaks at 1608, 1628, 1639, 1655, and 1692 cm^{-1} plus a shoulder at 1670 cm^{-1} that corresponds to particular secondary structures previously documented. Absorbance at 1628 and 1639 cm^{-1} may be attributed to β sheets.^{25,26} Soy protein secondary structure in fact consists of $\sim 60\%$ β sheet.²⁷ Absorbance at 1655 cm^{-1} results from either α -helix or random coil structures, whereas 1670 and 1692 cm^{-1} correspond to β turns.²⁸ The small absorbance at 1608 cm^{-1} is believed to be due to amino acid side-chain residue vibration.

The spectra of pure SPI microspheres and those of native SPI were similar except for a strong band appearing at 1622 instead of 1628 cm^{-1} , suggesting reorganization of the polypeptide chain after particle formation and domination of the intermolecular β -sheet within the microsphere networks. The

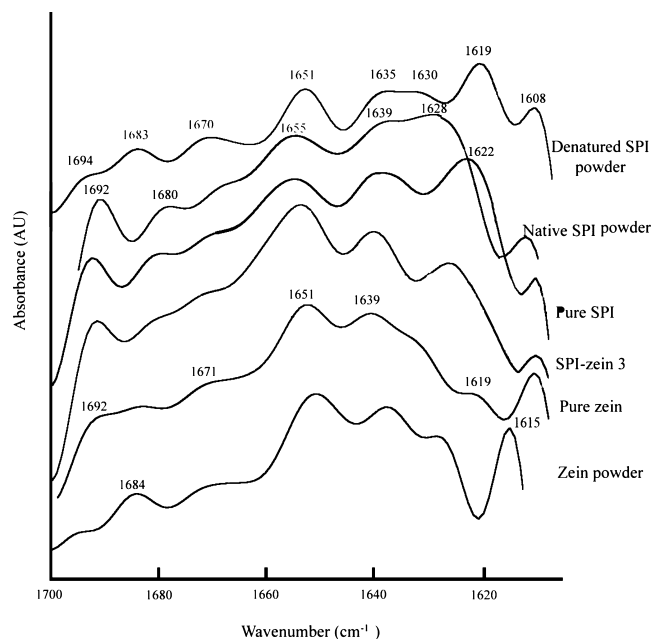


Figure 2. FTIR spectra of native proteins and SPI/zein microspheres.

formation of the intermolecular β sheet thus appears to be a key event in the aggregation of denatured SPI and is consistent with the cold gelation mechanism suggested for SPI hydrogels.¹⁵

The amide I band of zein is composed of five major absorbance peaks. Absorbance at 1628, 1638, 1650, and 1691 cm^{-1} corresponds to β -sheet, unordered structure, α helix, and β turn, respectively.²⁹ Absorbance at 1615 cm^{-1} may be a combination of activities at 1608 and 1619 cm^{-1} , suggesting intermolecular β -sheet structure and amino acid side-chain residues vibration. Strong absorption at 1650 cm^{-1} indicates that the α helix dominated, although a contribution of unordered structures cannot be ruled out, which is consistent with previous reports.^{30,31} After particle formation, absorbance at 1650 cm^{-1} increased, whereas absorbance at 1628 cm^{-1} decreased, indicating strengthening of α -helix structure in the microsphere networks. The spectra of microspheres made by blending equal amounts of SPI and zein (SPI-zein-3) displayed contributions from both proteins, and the α helix seemed to dominate. Blends containing 80 and 60% SPI gave similar spectra (not shown), although β -sheet absorbance (1628 cm^{-1}) increased with SPI content, whereas α -helix absorbance (1650 cm^{-1}) increased with zein content.

XRD patterns of the microspheres as well as SPI and zein prior to particle formation are shown in Figure 3. Pure zein microspheres show peaks at 4.6 and 10 Å (Figure 3a), as has been reported for zein films,³² suggesting similar protein aggregate structures for these two forms. The smaller d spacing (4.5 Å) arises mainly from the α -helix structure of zein, whereas the longer d spacing (10 Å) is thought to come from lateral α -helix packing. Matsushima et al. and Lai et al. have suggested a spatial structure model for zein that contains 9 or 10 successive helical segments.^{33,34} The helices are folded upon each other in antiparallel fashion, linked at each end by glutamine-rich turns or loops, and stabilized by hydrogen bonds. Subunits of neighboring zein molecules are then packed in hexagonal array (the monomer prisms of a zein molecular aggregate are staggered by one radius with respect to each other). In this case, 10–14 Å spacings were considered to be reasonable for the average distance between zein helical axes within an aggregate

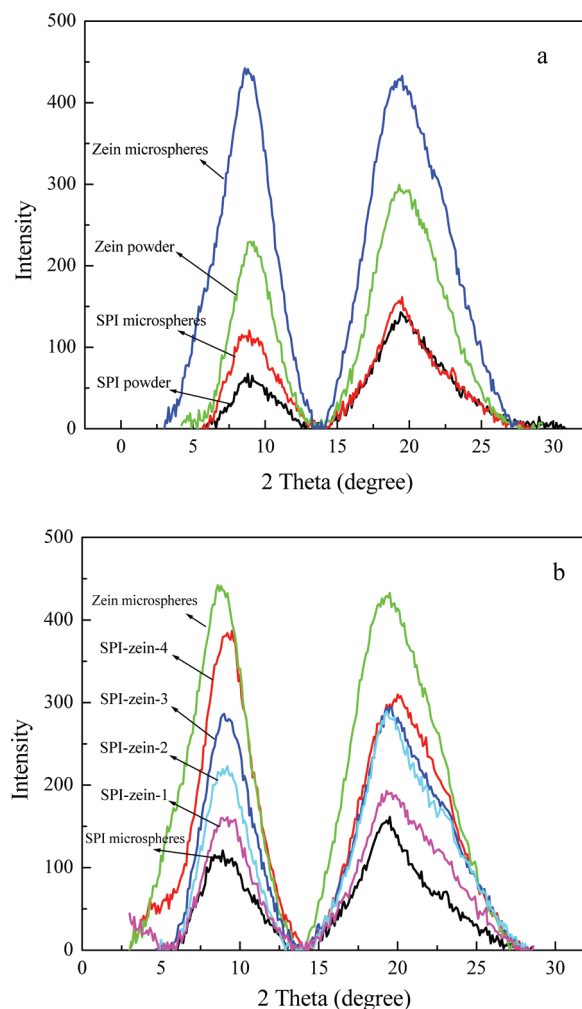


Figure 3. X-ray diffraction patterns of (a) pure SPI and pure zein microspheres and dried native protein and (b) microspheres at various SPI/zein ratios. (See the Supporting Information Section S1.)

depending on the size of the side chains. Pure SPI microspheres show peaks at 4.7 and 10 Å, similar to the XRD patterns of soy protein films.³⁵ However, the interpretation of XRD data in terms of soy protein aggregate structure is lacking. The d spacings at 4.7 and 10 Å may be attributed, respectively, to SPI β -sheet and intermolecular β -sheet packing on the basis of our FTIR spectra and on XRD patterns reported for other proteins (Li, L.; Darden, T. A.; Bartolotti, L.; Kominos, D.; Pedersen, L. G., 1999; Athamneh, Barone, 2008).^{36,37}

In the case of SPI microspheres, enhanced diffraction intensity at 10 Å suggested that intermolecular β -sheet content increased after SPI cold gelation, whereas for zein microspheres, intensity increased significantly at 4.5 Å and especially at 10 Å, implying postgelling increases in both α -helix backbone and molecular aggregate content. The overall greater intensity indicates that zein has a more crystalline structure than SPI. In the blended microspheres (Figure 3b), the increasing diffraction intensities reflected zein content, especially at 4.5 to 4.7 Å, suggesting good compatibility of the two proteins as well as the greater crystallinity of zein. Because no phase-separation was observed, it may be assumed that despite being hydrophobic, zein is miscible with amorphous regions of soy protein. Our results suggest that adjusting the SPI/zein ratio not only modifies the matrix hydrophobic/hydrophilic balance, as expected, but might also provide simple means of modifying the nutrient release properties of the microspheres because the effects of polymer

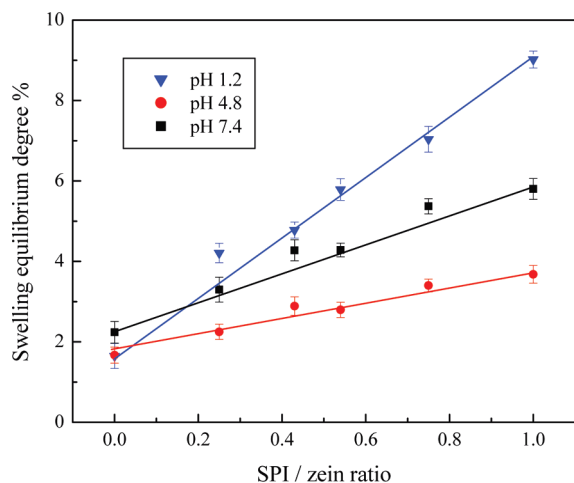


Figure 4. Swelling of SPI/zein microspheres at equilibrium at different pH.

matrix crystallinity on payload ingredient release kinetics have been reported.³⁸

3.3. Swelling Properties. Consisting primarily of amphoteric polyelectrolytes containing both cationic and anionic fixed charges, pure SPI microspheres showed typical polyampholyte hydrogel characteristics, exhibiting swelling in response to external pH conditions,³⁹ as depicted in Figure 4. Swelling reached equilibrium within 15–20 min (data not shown), indicating rapid penetration of buffer because of the small size of the spheres and the hydrophilic nature and amorphous structure of the matrix. Swelling was minimal near the isoelectric point (pI) and greater at pH 1.2 or pH 7.4, suggesting that swelling behavior is governed mainly by the net charge of the protein molecules. Near the pI, the numbers of $-\text{NH}_3^+$ and $-\text{COO}^-$ groups on the polypeptide chains are presumed to be nearly equal, and few ionized groups are free to repel each other. At pH 1.2, the chains bear a strong positive net charge due to $-\text{NH}_3^+$ groups, whereas at pH 7.4, they bear a strong negative net charge because of $-\text{COO}^-$ groups. The resulting electrostatic repulsion allowed the buffer to diffuse into the protein network. The swelling was greater at pH 1.2 than at 7.4, which is the opposite of the results obtained for SPI film in our previous work.⁴⁰ Because soy protein is rich in glutamic acid (11.9%) and aspartic acid (20.5%)⁴¹ and hence $-\text{COOH}$ groups, repulsive electrostatic forces and hence infiltration of the SPI interchain space by buffer should be greater at pH 7.4. However, in cold-gelled microspheres, most of the $-\text{COO}^-$ groups were involved in electrostatic interaction with Ca^{2+} , and the net negative charge at pH 7.4 was therefore small compared with the net positive charge resulting from amino groups at pH 1.2.

In contrast, zein microspheres were not sensitive to pH changes and swelled little in both simulated gastric and intestinal buffers. Under equilibrium conditions, the hydration capability of a polymer matrix is governed mainly by its hydrophilicity or crystallinity³⁸ because water molecules adsorb to amorphous regions but much less to crystalline regions. Zein is rich in hydrophobic residues such as leucine, proline, alanine, and phenylalanine. Although the two opposite surfaces that are rich in glutamine turns or loops are considered polar, the elongated prismlike model has a large hydrophobic surface in the *ac* plane, which forms a strong barrier against buffer permeation.⁴² The highly crystalline structure of the zein aggregates inside the microspheres no doubt prevents appreciable buffer uptake within the period of observation in this study.

Unlike pure SPI or zein matrices, the blended protein microspheres swelled gradually and reached equilibrium after

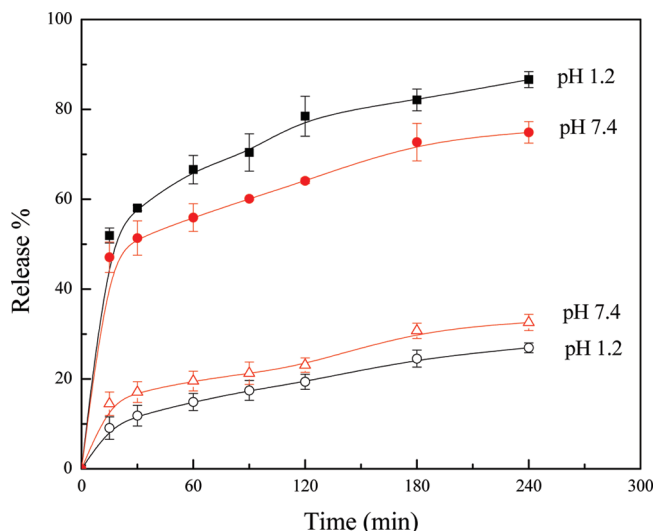


Figure 5. Release of riboflavin from pure SPI (solid symbol) and pure zein (hollow symbol) microspheres in simulated gastric (pH 1.2) and intestinal (pH 7.4) fluids.

3 h (data not shown). This swelling behavior can be attributed to gradual penetration of the buffer into the amorphous region of the matrix. It is encouraging to find that the degree of swelling of SPI/zein microspheres at equilibrium increased with increasing SPI/zein ratio at all pH values tested, and a linear relationship ($r^2 > 0.976$) between these two parameters was observed. SPI is composed of hydrophilic polypeptides with flexible molecular chains, whereas zein is composed of hydrophobic polypeptides with strong crystalline structure, according to XRD data. The increase in hydrophobic and crystalline regions inside the microspheres as zein content increased probably explains the decreased protein matrix hydration. In addition, with decreasing SPI/zein ratio, the swelling behavior of the blended protein microspheres became less sensitive to pH because of the decrease in hydrated $-\text{COO}^-$ and $-\text{NH}_3^+$ groups and associated increase in matrix hydrophobicity and crystallinity. Blending of SPI and zein thus appears to provide a convenient method of controlling microsphere swelling. Because hydration is one of the most important parameters to regulate release properties of the protein matrices according to our previous work, this modulated swelling may lead to controlled release behavior of the SPI/zein microspheres.

3.4. Nutrient Incorporation and Controlled Release. The release properties of the protein microspheres were investigated in simulated gastric and intestinal fluids using riboflavin as a nutrient model. Riboflavin is a water-soluble vitamin involved in vital metabolic processes in the body and is necessary for normal cell function, growth, and energy production. An EE of 79–88% was obtained for all microspheres, with LE ranging from 9.0 to 9.8%, as shown in the Supporting Information (Section S1). Microscopic observation revealed uniform distribution of riboflavin throughout the microsphere networks (image not shown). Riboflavin losses occurred mainly during washing of the microspheres. Because riboflavin is a low-molecular-weight water-soluble vitamin with no strong interaction with SPI or zein, its diffusion was inevitable.

Figure 5 shows the profile of riboflavin release from pure SPI and zein microspheres over time in gastric (pH 1.2) and intestinal (pH 7.4) medium. A two-phase pattern of release was observed for SPI microspheres, exhibiting a rapid burst release in both gastric and intestinal medium for the first 15 min of the test, followed by steady release from 15 min to 4 h with near zero-order release kinetics ($r^2 > 0.991$). The first phase represents

events during the time needed for swelling of the dry SPI microspheres in the release medium (in agreement with the swelling data) and corresponds to the release of ~50% of the nutrient within 15 min. In this process, the SPI matrices changed to a gel state upon interaction with the solvent. The protein molecular chains in the gel state, being more mobile than in the dry state, allow the active agent to diffuse out of the matrix. Faster release in simulated gastric buffer than in simulated intestinal buffer was observed, which can be attributed to greater swelling of the SPI microspheres at pH 1.2. Clearly, early burst release is undesirable in controlled delivery applications, suggesting that soy protein should not be used alone as coating material for controlled release of hydrophilic nutrients like riboflavin because of their low barrier capacity on the micrometer scale.

In contrast, riboflavin was released slowly in both simulated gastric and intestinal buffer from zein microspheres of similar size. The release profile also followed a two-phase pattern, that is, burst release of 10–15% riboflavin during the first 15 min of the test, which can be attributed to vitamin entrapped near the surface of the microspheres, followed by a very slow release stage, resulting in only another 10–15% released after 4 h. The highly crystalline structure and hydrophobic nature of the zein microspheres explains this slow release. This structure prevented penetration and diffusion of the release medium into the zein matrix, leading to minimal particle swelling (shown in Section 3.3) and subsequent slow dissolving and release of riboflavin. The very similar release profiles at both pH 1.2 and 7.4 reflected the insensitivity of zein matrix swelling to medium pH changes, as demonstrated in Section 3.3. It should be emphasized that too low of a release rate is also undesirable for oral delivery because of the decrease in nutrient utilization.

It is interesting to find that nutrient release rates can be controlled by adjusting the SPI/zein ratio, as shown in Figure 6a,b. The riboflavin release rate decreased progressively with increasing zein content, which may be attributed to the resulting increased hydrophobicity and crystallinity and hence decreased rate of hydration of the microspheres. Release in simulated gastric fluid was faster from microspheres with SPI/zein ratios of 8:2, 6:4, and 5:5. Less than 20% of the riboflavin was released from microspheres with SPI/zein ratios of 5:5 and 3:7 after 30 min in gastric fluid, which is the expected time for a food product to pass from the stomach into the intestine and suggests that most of the payload could reach the intestine without being exposed to gastric conditions. Furthermore, these same microspheres showed near-zero-order release kinetics in the simulated intestinal fluid, resulting in 40–60% release of the riboflavin after 4 h of the test. The remaining riboflavin was analyzed after complete enzymatic degradation of the protein matrices and found 91–96% active, indicating that the nutrient was well preserved in the microspheres. It is expected that complete riboflavin release would be achieved over 8–10 h. Overall, SPI/zein-3 and SPI/zein-4 demonstrated the greatest potential for use as delivery systems for nutraceutical products in functional foods.

3.5. Nutrient Release Mechanisms. Efficient and reproducible design of systems for controlled delivery of nutraceutical products will require increased understanding of the release mechanisms. The Korsmeyer–Peppas semiempirical equation⁴³ was applied to identify the mechanism of riboflavin release from the protein microspheres

$$M_t/M_\infty = kt^n \quad (2)$$

where M_t/M_∞ is the fraction of core released after time t relative to the amount of core released at infinite time, k is a constant,

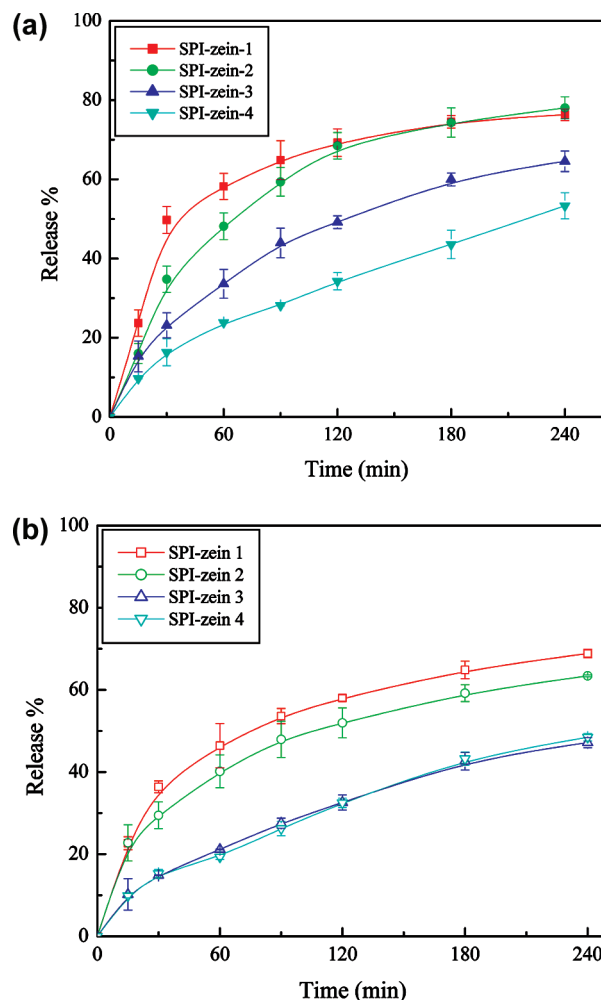


Figure 6. (a) Release of riboflavin from SPI/zein microspheres in simulated gastric fluid. (b) Release of riboflavin from SPI/zein microspheres in simulated intestinal fluid.

and n is the diffusional exponent. Inferences about the release mechanism are based on the fit of this equation to the drug release data through 60% dissolution and comparison of the value of n to the semiempirical values reported by Peppas. For spherical particles, $n = 0.43$ indicates Fickian diffusion, $0.43 < n < 0.85$ indicates anomalous (non-Fickian) transport, and $n = 0.85$ indicates case II transport. The results of the above calculations are included in the Supporting Information (Section S2). Pure zein microspheres showed n values of 0.47 and 0.43 at pH 1.2 and 7.4, respectively, after the 15 min burst release period, indicating Fickian diffusion of the incorporated nutrient, whereas pure SPI microspheres and SPI/zein-1 (8:2) showed n values of 0.23 to 0.31. Peppas et al. attributed n values this low to core ingredient release through water-filled pores⁴⁴ or to broad distribution of particle size.⁴⁵ However, TEM photographs showed continuous structure, and Mastersizer analysis showed rather narrow particle size distribution for these SPI-rich microspheres. The 15 min burst release, followed by the gradual release of the remaining riboflavin may explain these low n values, which correspond to the smallest release profile curvatures. PI/zein microspheres at ratios of 6:4, 5:5, or 3:7 gave n values ranging from 0.49 to 0.59 in simulated gastric and intestinal fluids, indicating anomalous transport involving both riboflavin diffusion and protein matrix relaxation mechanisms. The n value of 0.59 obtained at a SPI/zein ratio of 3:7 was the highest obtained. The n value decreased with increasing SPI content, suggesting that protein molecule relaxation may

contribute to nutrient release from microspheres with a higher zein content. As suggested by the swelling data, both release media (pH 1.2 and 7.4) appear to penetrate SPI-rich matrices much more easily because of their hydrophilic nature and amorphous structure, inducing protein chain relaxation quickly and causing matrix swelling to reach equilibrium within 15 min, followed by riboflavin dissolution and diffusion. In this case, diffusion of nutrient dominated the entire release process. For SPI/zein-2 (6:4), n is not far from 0.43, indicating an almost Fickian diffusion. In microspheres containing more zein, release media penetrated the amorphous regions much more slowly, thus inducing more gradual relaxation of the polypeptide chains and making particle swelling the principal mechanism of nutrient release. In this process, both diffusion and polymer relaxation regulate nutrient release.

To obtain further clarification of the contribution of Fickian diffusion and polymer relaxation to nutrient release, the data were fitted to the equation proposed by Gander et al.⁴⁶

$$M_t/M_\infty = k_1 t^{1/2} + k_2 t \quad (3)$$

where the k_1 and k_2 are, respectively, the nutrient diffusional and polymer relaxational constants. As shown in the Supporting Information (Section S2), the relative contributions of Fickian diffusion and polymer relaxation to nutrient release are very evident from the values of k_1 and k_2 . The influence of diffusion was always stronger than that of polymer relaxation, indicating that core diffusion plays a major role in regulating the release of the nutraceutical payload.

The diffusion coefficient, D , for the transport of aqueous nutrient solution from the microspheres was calculated according to the equation of Crank⁴⁷

$$D = (r \times \theta / (6 \times M_\infty))^2 \times \pi \quad (4)$$

where θ is the slope of the linear portion of the plot of M_t/M_∞ versus $t^{1/2}$, r is the radius of the microspheres, and M_∞ is release at equilibrium. The values of D are also presented in the Supporting Information (Section S2). They range from $(4.7\text{--}6.8) \times 10^{-8}$ cm²/s for pure SPI microspheres, which is similar to those of alginate interpenetrating network (IPN) beads with gelatin or egg albumin cross-linked by glutaraldehyde $((3.32\text{--}9.11) \times 10^{-8}$ cm²/s) but lower than those for pure alginate beads $((2.1\text{--}5.4) \times 10^{-6}$ cm²/s).⁴⁸ The D value decreased as the zein content increased because of increased hydrophobicity and crystallinity. It can be concluded that by setting the SPI/zein ratio, the protein matrix diffusion coefficient can be adjusted to induce different swelling behaviors and subsequent nutrient release profiles, considering that diffusion is the major nutraceutical release mechanism. Natural polymers such as alginate, gelatin, and soy protein have good biocompatibility and biodegradability, making them suitable as food microencapsulation materials. However, they generally exhibit rapid hydrophilic core release on the micrometer scale because of the low barrier capacity associated with their hydrophilic nature, which limits their applications. In this work, microspheres with SPI/zein ratios of 5:5 and 3:7 had much better barrier capacities than pure SPI microspheres, corroborated by their lower D values $((2\text{--}5.6) \times 10^{-9}$ cm²/s), which led to near zero-order release of the model nutraceutical payload. These SPI/zein microspheres thus show potential for use as nutraceutical delivery systems.

4. Conclusions

The strategy of blending SPI and zein provided a convenient method for varying the diffusion coefficients and hence the

swelling behavior and nutrient release kinetics of food-protein-based microspheres in simulated gastrointestinal fluids. The diffusion mechanism plays a major role in regulating the release of hydrophilic nutrients such as riboflavin from protein microspheres. Microspheres with SPI/zein ratios of 5:5 and 3:7 displayed near-zero-order release kinetics in the simulated gastrointestinal environment and thus show potential for use as delivery systems for nutraceutical products in functional foods.

Acknowledgment. This study was funded by the Canada Research Chairs Program (M. Subirade), the Natural Sciences and Engineering Research Council of Canada (NSERC), and the Canadian Institute of Health Research (CIHR) (Collaborative Health Research Projects program).

Supporting Information Available. Tables showing particle size and riboflavin encapsulation values of SPI/zein microspheres and kinetics of riboflavin release from SPI/zein microspheres. This material is available free of charge via the Internet at <http://pubs.acs.org>.

References and Notes

- Gharsallaoui, A.; Roudaut, G.; Chambin, O.; Voille, A.; Saurel, R. *Food Res. Int.* **2007**, *40*, 1107.
- Peppas, N. A.; Bures, R.; Leobandung, W.; Ichikawa, H. *Eur. J. Pharm. Biopharm.* **2000**, *50*, 27.
- Langer, R.; Peppas, N. A. *AIChE J.* **2003**, *49*, 2990.
- Chen, L.; Remondetto, G. E.; Subirade, M. *Trends Food Sci. Tech.* **2006**, *17*, 272.
- Chen, L.; Subirade, M. Chapter 10: Food-Protein-Derived Materials and Their Use as Carriers and Delivery Systems for Active Food Components. In *Delivery and Controlled Release of Bioactives in Foods and Nutraceuticals*; Garti, N., Ed.; Woodhead Publishing: Cambridge, U.K., 2008.
- Chen, L.; Remondetto, G. E.; Subirade, M. Chapter 6: Calcium Cross-Linked Soy Protein Beads and Microspheres for Nutraceutical Compound Delivery. In *Micro/Nanoencapsulation of Active Food Ingredients*; Huang, Q.; Given, P.; Qian, M., Eds.; American Chemistry Society Symposium Series 1007; American Chemical Society: Washington, D.C., 2009.
- Chen, L. In *Designing Functional Foods: Understanding, Measuring, and Controlling Food Structure Breakdown and Nutrient Absorption for the Development of Health-Promoting Foods*; McClements, D. J., Decker, E., Eds.; Woodhead Publishing: Cambridge, U.K., 2009.
- Beaulieu, L.; Savoie, L.; Paquin, P.; Subirade, M. *Biomacromolecules* **2002**, *3*, 2239.
- Chen, L.; Subirade, M. *Biomaterials* **2005**, *26*, 6041.
- Chen, L.; Subirade, M. *Biomaterials* **2006**, *27*, 4646.
- Chen, L.; Subirade, M. *Eur. J. Pharm. Biopharm.* **2007**, *65*, 354.
- Saio, K.; Watanabe, T. *J. Texture Studies* **1978**, *9*, 135.
- Maltais, A.; Remondetto, G. R.; Gonzales, R.; Subirade, M. *J. Food Sci.* **2005**, *70*, 67.
- Barbut, S.; Foegeding, E. A. *J. Food Sci.* **1993**, *58*, 867–871.
- Maltais, A.; Remondetto, G. E.; Subirade, M. *Food Hydrocolloids* **2008**, *22*, 4550.
- Maltais, A.; Remondetto, G. E.; Subirade, M. *Food Hydrocolloids* **2009**, *23*, 1647.
- Zheng, H.; Zhou, Z.; Chen, Y.; Huang, J.; Xiong, F. *J. Appl. Polym. Sci.* **2007**, *106*, 1034.
- Gan, C. Y.; Cheng, L. H.; Easa, A. M. *Innovative Food Sci. Emerging Technol.* **2008**, *9*, 563.
- Gouin, S. *Trends Food Sci. Tech.* **2004**, *15*, 330.
- Champagne, C. P.; Fustier, P. *Curr. Opin. Biotech.* **2007**, *18*, 184.
- Lazko, J.; Popineau, Y.; Renard, D.; Legrand, J. J. *Microencapsulation* **2004**, *21*, 59.
- Corradini, E.; Mattoso, L. H. C.; Guedes, C. G. F.; Rosa, D. S. *Poly. Adv. Tech.* **2004**, *15*, 340.
- Kim, S.; Sessa, D. J.; Lawton, J. W. *Ind. Crops Prod.* **2004**, *20*, 291.
- Preparation of Solid Surfaces. In *Interfacial Forces in Aqueous Media*; Van Oss, C. J., Ed.; Marcel Dekker: New York, 1994.
- Arrondo, J. L. R.; Muga, A.; Castresana, J.; Goni, F. M. *Prog. Biophys. Mol. Biol.* **1993**, *59*, 23.
- Lefèvre, T.; Subirade, M. *Biopolymers* **2000**, *54*, 578.

- (27) Hwang, D. C.; Damodaran, S. *J. Agric. Food Chem.* **1996**, *44*, 751.
- (28) Caillard, R.; Remondetto, G. E.; Subirade, M. *Food Res. Int.* **2009**, *42*, 98.
- (29) Boye, J. I.; Ismail, A.; Alli, I. *J. Dairy Res.* **1996**, *63*, 97.
- (30) Mejia, C. D.; Mauer, L. J.; Hamaker, B. R. *J. Cereal Sci.* **2007**, *45*, 353.
- (31) Mizutani, Y.; Matsumura, Y.; Imamura, K.; Nakanishi, K.; Mori, T. *J. Agric. Food Chem.* **2003**, *51*, 229.
- (32) Wang, Y.; Filho, F. L.; Geil, P.; Padua, G. *Macromol. Biosci.* **2005**, *5*, 1200.
- (33) Matsushima, N.; Danno, G. I.; Takezawa, H.; Izumi, Y. *Biochem. Biophys. Acta.* **1997**, *1339*, 14.
- (34) Lai, H. M.; Geil, P. H.; Padua, G. W. *J. Appl. Polym. Sci.* **1999**, *71*, 1267.
- (35) Wu, Q.; Zhang, L. *Ind. Eng. Chem. Res.* **2001**, *40*, 1879.
- (36) Li, L.; Darden, T. A.; Bartolotti, L.; Kominos, D.; Pedersen, L. G. *Biophys. J.* **1999**, *76*, 2871.
- (37) Athmaneh, A.; Griffin, M.; Whaley, M.; Barone, J. R. *Biomacromolecules* **2008**, *9*, 3181–3187.
- (38) Frank, A.; Rath, S. K.; Venkatraman, S. S. *J. Controlled Release* **2005**, *102*, 333.
- (39) Chen, L.; Tian, Z.; Du, Y. *Biomaterials* **2004**, *25*, 3725.
- (40) Chen, L.; Remondetto, G. E.; Rouabhia, M.; Subirade, M. *Biomaterials* **2008**, *29*, 3750.
- (41) Krochta, J. M.; De Mulder-Johnston, C. D. *Food Technol.* **1997**, *51*, 61.
- (42) Wang, Q.; Crofts, A. R.; Padua, G. W. *J. Agric. Food Chem.* **2003**, *51*, 7439.
- (43) Ritger, P. L.; Peppas, N. A. *J. Controlled Release* **1987**, *5*, 37.
- (44) Peppas, N. A. *Macromolecules* **1985**, *33*, 3530.
- (45) Ritger, P. L.; Peppas, N. A. *J. Controlled Release* **1987**, *5*, 23.
- (46) Gander, B.; Gurny, R.; Doelker, E.; Peppas, N. A. *J. Controlled Release* **1998**, *5*, 271.
- (47) Crank, J. *The Mathematics of Diffusion*, 2nd ed.; Crank, J., Ed.; Clarendon Press: Oxford, U.K., 1975.
- (48) Kulkarnia, A. R.; Soppimatha, K. S.; Aminabhavia, T. M.; Rudzinski, W. E. *Eur. J. Pharm. Biopharm.* **2001**, *51*, 127.

BM900989Y